International Symposium on Air & Water Pollution Abatement Catalysis (AWPAC) – Catalytic pollution control for stationary and mobile sources

Photo-Fenton oxidation of phenol over a Cu-doped Fe-pillared clay

Haithem Bel Hadjltaief [a], Mourad Ben Zina [a], Maria Elena Galvez [b,c,*], Patrick Da Costa [b,c]

[a] Laboratoire Eau, Énergie et Environnement (LR3E), Code: AD-10-02, École nationale d'ingénieurs de Sfax, Université de Sfax, BP1173.W.3038 Sfax, Tunis, Tunisia
[b] Université Paris-6, UPMC Sorbonne Universités, Institut Jean-Le-Rond-d'Alembert, 2, place de la Gare-de-Ceinture, 78210 Saint-Cyr-l'École, France
[c] Institut Jean-Le-Rond-d'Alembert, UMR CNRS 7190, 2, place de la Gare-de-Ceinture, 78210 Saint-Cyr-l'École, France

ARTICLE INFO

ABSTRACT

A Cu-doped Fe-pillared Tunisian clay (Cu/Fe–PILC) was synthesized and used as a catalyst in the heterogeneous photo-Fenton oxidation of phenol in aqueous solution. Textural, structural and chemical characterization pointed to successful pillaring and incorporation of the Cu active phase. Photo-Fenton experiments proved the high activity of the Cu/Fe–PILC catalyst, which was able to completely mineralize the phenol present in the treated solution after a reaction time of 40 min and in the presence of UV-C light. Moreover, the catalytic activity was not influenced by the pH of the initial phenol solution, over a wide range of pH from 3 to 7. An optimal dosage of H_2O_2 and of the catalyst was found. Phenol degradation was found to be slower in the presence of UV-A irradiation, needing longer reaction times. Negligible metal leaching and catalyst reutilization without noticeable loss of activity point to an excellent catalytic stability for this Cu/Fe–PILC catalyst.

© 2015 Académie des sciences. Published by Elsevier Masson SAS. All rights reserved.

1. Introduction

Phenol-containing wastewater discharged from various industrial processes represent an important environmental hazard, since phenol can cause considerable damages to the ecosystem and human health, causing alterations to the central nervous system, liver, kidney and blood of humans and animals [1,2]. Considerable efforts have been therefore made in the last decades in order to find a technology that allows an effective removal of phenol from wastewaters at a reasonable cost [3].

With this aim, several advanced oxidation processes (AOPs) have been proposed to convert the organic pollutants in contaminated water into carbon dioxide or, at least, into less toxic substances [4]. Among the different AOPs, homogeneous Fenton and photo-Fenton reactions are considered one of the most efficient routes for the complete oxidation of recalcitrant chemicals in water [5–11]. The major drawback of Fenton oxidation is its low efficiency at neutral pH, due to the precipitation of iron compounds and to the deactivation of the main reactive radicals under such conditions [6,7]. In a similar way to iron, copper can also promote the Fenton reactions [7,9]. Although copper possesses lower catalytic activity than iron under acidic pH conditions, it exhibits higher

* Corresponding author. Université Paris-6, UPMC Sorbonne Universités, Institut Jean-Le-Rond-d'Alembert, 2, place de la Gare-de-Ceinture, 78210 Saint-Cyr-l'École, France.
E-mail addresses: elena.galvez_parruca@upmc.fr, megalvez@dalembert.upmc.fr (M.E. Galvez).

activity under circumneutral and alkaline pH conditions [9,10]. In both cases, the use of either iron or copper in homogeneous phase has important disadvantages, such as the need for the separation and regeneration of the catalyst and the possible secondary contamination due to its presence in the treated effluent. The replacement of the homogeneous catalyst by a heterogeneous system containing the active phase is therefore needed. Different porous materials, such as synthetic and natural zeolites, clays, polymers, silica, carbon or resins have been considered supports that contain and fix this active phase [8–10]. Among them, clay-based catalysts, i.e. ion-exchanged pillared clays, represent an interesting option for water treatment, due to the low cost and ready abundance of clays, their high resistance and stability, together with the simplicity of the pillaring process [12–17]. Concretely, copper-doped iron pillared clays have been recently shown to be considerably active and selective in Fenton-like processes [12,13]. In the present work, we aim at evaluating the photo-Fenton activity of an iron pillared Tunisian clay doped with copper oxides. The influence of different important reaction parameters, such as pH, type of irradiation, i.e. its wavelength, and concentration of catalyst and oxidant, has been considered. The stability of the catalyst has been as well examined in terms of metal leaching and catalyst reusability.

2. Experimental

2.1. Catalysts preparation

A natural clay from the deposit of Jebal Cherahil (Kairouan, Central–West region of Tunisia) was chosen as the raw material. The procedure for its purification and for the Na-ion exchange of its surface have been previously described elsewhere [11,18].

The Fe-pillared clay was synthesized as described in detail in our previously published work [18]. The pillaring solution was prepared by slow addition of Na_2CO_3 powder (97%, MERCK) into a 0.2 M solution of $Fe(NO_3)_3 \cdot (Fe(NO_3)_3 \cdot 9H_2O$ 97%, MERCK) under stirring at 100 rpm for 2 h at room temperature until the molar ratio Fe/Na_2CO_3 reached 1:5. The solution was then aged during four days at 60 °C. Finally, the resulting oligomeric Fe (III) solution was added into a 2 wt% aqueous dispersion of the purified Na-exchanged clay, at a ratio of 10^{-3} mol of Fe^{3+} per gram of clay. The dispersion was agitated at 100 rpm for 24 h, then filtered, washed with deionized water several times, and finally centrifuged at 4000 rpm for 10 min. The resulting solid material was calcined at 300 °C for 24 h, and subsequently ground to 100-mesh, in order to obtain the pillared clay, Fe–PILC. For the preparation of the Cu-doped catalyst, Cu/Fe–PILC, 1 g of Fe–PILC and 100 mL of a 0.02 M copper acetate $(Cu(CH_3COO)_2$ (98%) MERCK) solution were stirred at a pH of 5.2 and 40 °C for 24 h. The resulting suspension was filtered and the precipitate was washed several times with deionized water. The catalyst was then dried at 120 °C for 12 h and subsequently calcined at 400 °C for 5 h.

2.2. Physicochemical characterization

The chemical composition and structural features of the natural and modified clay were analyzed by means of X-ray fluorescence (XRF, ARL® 9800 XP spectrometer), powder X-ray diffraction (XRD Philips® PW 1710 diffractometer, Kα, 40 kV/40 mA, scanning rate of 2θ per minute) and infrared spectroscopy (IR, Digilab Excalibur FTS 3000 spectrometer). The textural properties of the different materials were evaluated by means of nitrogen adsorption at −196 °C (Micromeritics ASAP 2020). The morphology of the samples was studied using scanning electronic microscopy (SEM, Hitachi SU-70). The microscope was coupled with an Oxford X-Max 50-mm^2 energy dispersive X-ray detector, which enabled the qualitative evaluation of the chemical composition of the different materials.

2.3. Photo-Fenton catalytic experiments

The photo-Fenton catalytic oxidation experiments were carried out in a 250-mL Pyrex open vessel, water-cooled and placed on a magnetic stirrer under 2 parallel UV lamps 2×15 at 254 and 365 nm with 930/1350 μW/cm^2. The distance between the solution and the UV lamps was kept constant at 15 cm. All of the experiments were performed at room temperature, i.e. 25 °C. The initial pH of the different phenol solutions was kept at its natural value (around 5) and not modified except when noted. After stabilization of the stirring speed (150 rpm), the desired amount of Cu/Fe–PILC catalyst was added to 200 mL of an aqueous phenol solution (prepared using analytical-grade phenol 99%, Merck). Then, a fixed volume of a 1000 mg/L H_2O_2 solution (prepared from 35% H_2O_2, Merck; H_2O_2 solutions agitated in a thermostatic water-bath shaker for 60 min at 25 °C) was poured into the phenol solution. H_2O_2 addition was taken as the initial time of the reaction. Solution aliquots were periodically withdrawn from the reaction vessel with the aid of a syringe and at predetermined intervals. Residual H_2O_2 in these samples was immediately quenched with MnO_2 (99% Merck), in order to avoid the occurrence of dark Fenton-like reaction through the possible presence of leached iron or copper. Before analysis, the liquid was filtered using PTFE filters (0.45 μm).

The influence of several operational parameters on the degradation of phenol was studied. First, the influence of pH was considered. The solution pH was adjusted at pH = 3.5, 5.1 (natural pH of the initial phenol solution), and 7.1, using HCl (0.1 M) and NaOH (0.1 M), while fixing the phenol concentration at 150 mg/L and the dosages of H_2O_2 at 3 mL and 0.8 g/L of the Cu/Fe–PILC catalyst, corresponding to an H_2O_2 concentration of 0.44 mmol/L and to a molar ratio phenol/H_2O_2 equal to 3.6. The influence of the H_2O_2 amount added to the phenol solution was evaluated by varying its dosage range from 1 mL to 7 mL, i.e. molar ratios phenol/H_2O_2 from 1.5 to 10.8, at a fixed pH of 5.1 and a phenol concentration of 150 mg/L, in the presence of 0.8 g/L. The dosage of the catalyst was then varied from 0.1 to 1.5 g/L, for 150 mg/L of phenol solution, at pH = 5.1 and 2 mL of H_2O_2, i.e. a molar ratio phenol/H_2O_2 equal to 5.4.

The stability of the Cu/Fe–PILC catalysts was tested as well. Leaching runs were performed in order to evaluate
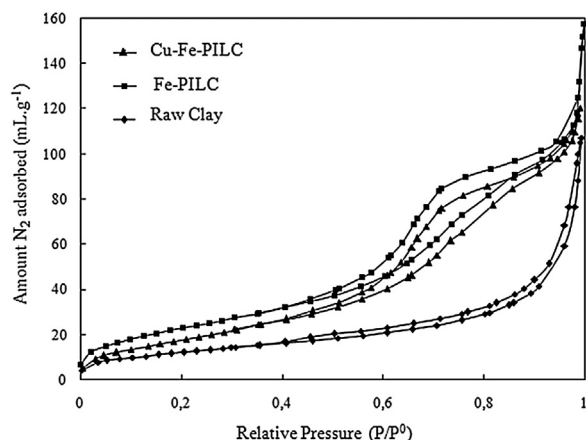
Fig. 1. Nitrogen adsorption–desorption isotherms for the raw clay, the iron pillared clay, and the Cu-doped pillared clay.

the catalytic activity of Cu/Fe–PILC during successive experiments and therefore assess the possibility of catalyst reuse. The catalysts were used in three consecutive experiments by using fresh phenol solutions at the concentration of 50 mg/L, pH 5.05, 2 mL of H_2O_2, and 0.6 g/L catalyst. Between each experiment, the catalyst was removed by filtration, then washed with distilled water several times, and dried at 110 °C for 12 h. The concentration of Fe and Cu ions solutions after reaction were analyzed by means of atomic absorption (ZEEnit 700 spectrometry, Analytik Jena).

The concentration of phenol in the solution was analyzed by means of gas chromatography (GC), in an Agilent 2025 GC equipped with a Zebron capillary column ZB-5MSi (30 m × 0.32 mm × 0.25 μm) and a flame ionization detector (FID). The extent of the mineralization of the phenol was determined on the basis of total organic carbon measurements using a Shimadzu TOC-5000A (Japan) analyzer.

Degradation efficiency and mineralization efficiency were calculated as follows:

$$\text{Degradation/mineralization efficiency} = (C_0 - C_t)/C_0 \times 100 \qquad (1)$$

where C_t and C_0 denote the time-dependent concentration/TOC and the initial concentration/TOC, respectively.

In order to complete the information on the oxidation process of phenol, additional analyses of the liquid samples extracted from the reaction vessel were performed by means of high-pressure liquid chromatography (HPLC, VARIAN), equipped with an electronic injector JASCO and a

PURSUIT 5 C18 150 × 4.6 mm column, with a detection wavelength of 254 nm under water and acetonitrile and a total flow rate of 0.5 mL/min.

3. Results and discussions

3.1. Characterization of the catalyst

The nitrogen adsorption isotherms for the raw clay, the pillared clay, Fe–PILC, and the Cu-doped pillared clay, Cu–Fe–PILC, are presented in Fig. 1. Whereas the adsorption isotherm obtained for the raw clay is indicative of its non-porous structure, nitrogen adsorption for both Fe–PILC, Cu–Fe–PILC Fe follows a type-IV isotherm (IUPAC) with a tight hysteresis loop at high relative pressures, $p/p_0 = 0.4$–1.0, which points to the presence of mesopores. The values of the BET surface area (S_{BET}), pore volume and average pore diameter calculated from the adsorption isotherms are summarized in Table 1. The BET surface area increases from 64 m^2/g to 149 m^2/g as a consequence of the pillaring process. However, upon copper addition, a slight decrease in the surface area of the catalyst can be observed, pointing to a certain extent of pore blockage. In any case, the values of the surface area are very similar to those previously reported for similar catalysts [16,18,19].

Table 1 contains as well the XRF results for the analysis of the chemical composition of the different materials. The iron oxide content in the pillared clay considerably increases with respect to the raw clay, due to the formation of the iron 'pillars' [18,20,21]. The copper oxide content increases from 0 to 11.1% upon Cu-loading, pointing to a successful impregnation of Fe–PILC with copper compounds.

The XRD patterns acquired for the raw clay, Fe–PILC and Cu/Fe–PILC catalysts are shown in Fig. 2. The XRD pattern for the raw clay evidences the presence of smectite (montmorillonite) associated with illite and kaolinite. Upon pillaring, the d-spacing calculated for the smectite phase increases from 14.5 Å in the raw clay to 19.3 Å. No copper oxide phases are observed in the XRD patterns acquired for the Cu-doped pillared clay, which points to a high dispersion of the CuO phase on the pillars of the Fe–PILC [12,13,22]. The reflections at $2\theta = 24.2°$, 30.6°, 32.4∘, 38.5°, 41.3°, 48.6° and 56.2° are related to the α-Fe_2O_3 phase, i.e. magnetite (JCPDS: 19-0629), whereas those at $2\theta = 35.5$, 43, 57 and 62.5° correspond to Fe_3O_4 [19,23,24], i.e. hematite (JCPDS card No. 33-0664).

Fig. 3 presents the FT–IR spectra recorded in transmission mode for the raw clay, the pillared clay and the Cu-catalyst. The three bands at 3443, 3600 and 3650 cm^{-1} are due to the O–H stretching in Al–OH in the inner hydroxyl

Table 1

Chemical composition (XRF), LOI (loss on ignition), and textural properties (N_2 adsorption) of the raw clay, the iron pillared clay, and the Cu-doped pillared clay.

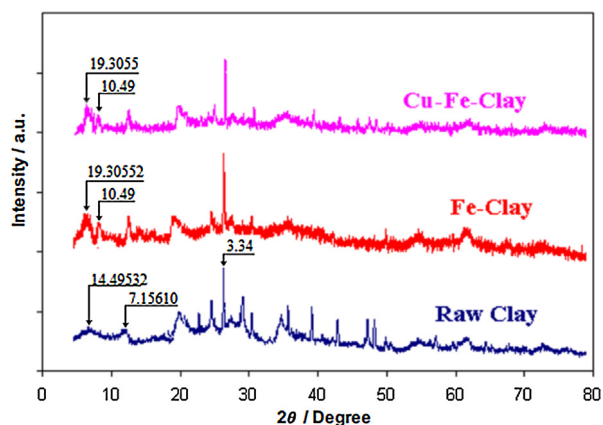| Oxides (%) | Chemical composition | | | | | | | | Textural properties | | | |
	SiO_2	Al_2O_3	Fe_2O_3	CaO	MgO	Na_2O	K_2O	CuO	LOI	V_p (cm^3/g)	P_d (nm)	S_{BET} (m^2/g)
Raw clay	42.4	16.82	7.7	4.9	4.5	2.5	0.5	–	18.17	0.19	3.7	64
Fe–PILC	38.5	17.61	18.81	1.5	1.8	1.56	0.65	–	13.8	0.38	3.90	143.4
Cu–Fe–PILC	37.0	17.32	17.91	0.8	1.5	1.61	0.01	11.1	12	0.36	3.82	119.6

Fig. 2. (Color online.) XRD patterns for the raw clay, the iron pillared clay and the Cu-doped pillared clay.

groups lying between the tetrahedral and octahedral sheets of the clay mineral [25]. The band appearing at $1428 cm^{-1}$ points to the presence of carbonates, i.e. calcite ($CaCO_3$) or dolomite ($Ca,Mg(CO_3)_2$), confirmed by the presence of CaO and MgO revealed by XRF analyses. The typical bands for the silicate components of the clay appear between 1200 and $400 cm^{-1}$, concretely one at $1047 cm^{-1}$, due to in-plane band stretching of Si–O bonds, and the second one at $513 cm^{-1}$, corresponding to Si–O–Si vibrations. The bands at 472 and $533 cm^{-1}$ can be assigned to Si–O–Mg and Si–O–Al species, respectively [25,26]. The spectra for the modified clays evidence a decrease in the intensity of the band at around $1430 cm^{-1}$, arising from the dehydration and dehydroxylation steps during the pillaring and after calcination. The absorption band at $935 cm^{-1}$ confirms the presence of dioctahedral smectite with AlAl–OH, AlFe–OH and AlMg–OH bending vibrations [16,27]. The FT–IR spectra, however, do not provide any direct evidence of the successful incorporation of Cu and Fe to the clay, or about the state of this metal species of the clay surface and/or structure.
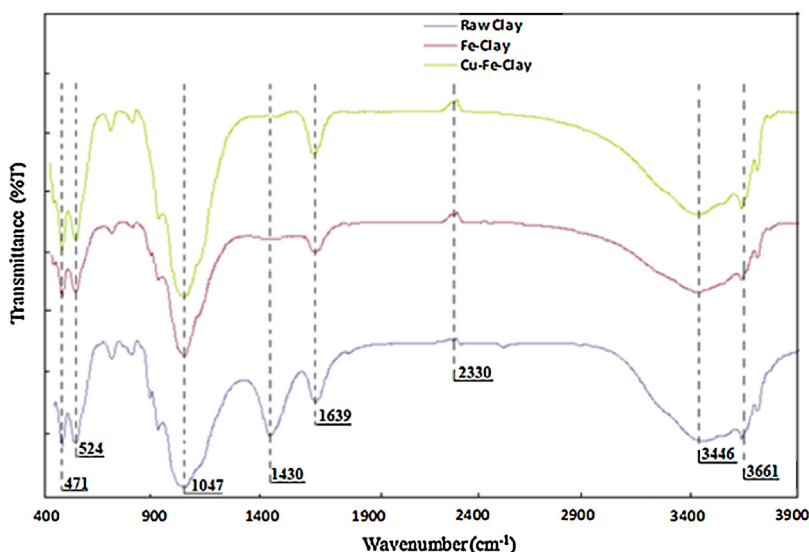
SEM observation of the different materials reveals that the surface morphology of the raw clay is different from that of Fe–PILC and of Cu/Fe–PILC (Fig. 4). The raw clay presents cornflake-like crystals on its surface with a fluffy appearance, revealing its extremely fine platy structure. Upon pillaring the Fe–PILC, and also in the case of the Cu/Fe–PILC catalyst, the surface becomes notably more porous and fluffy. EDS analysis confirmed the presence of both Fe and Cu on the pillared clays. Let us note here that the physicochemical characterization performed for the prepared catalysts does not show any clear evidence of the formation of Cu-pillars, and suggest only the deposition of a cooper oxide phase on the surface of the Fe-pillared clay.

3.2. Catalytic performance in the photo-Fenton oxidation of phenol

Fig. 5 shows the degradation of phenol, measured by means of gas chromatography, as a function of the reaction time, under different experimental conditions. In this experiment, the dose of H_2O_2 and the amount of Cu/Fe–PILC catalyst were respectively fixed at 3 mL (H_2O_2 concentration of 0.44 mmol/L) and 0.8 g/L. As expected, the sole presence of UV_{254} irradiation results in almost zero conversion, see curve (a). In the presence of the Cu/Fe–PILC catalyst, curve (b), a maximal phenol conversion around 22.1% was measured, which stabilizes after a reaction time of 90 min. This phenol conversion can be mostly ascribed to its adsorption on the clay surface (corresponding to an adsorption capacity of around 30 mg of phenol per gram of catalyst), though to some extent phenol oxidation in the presence of this catalyst might not be neglected. When H_2O_2 is added to the reactant mixture, either in the absence, curve (c), or in the presence, curve (d), of the Cu/Fe–PILC catalyst, phenol conversion increases, reaching 65.7% and 80.8%, respectively, after only 20 min of reaction. The highest conversion in the presence of the Cu-doped pillared clay confirms its catalytic activity and ability to promote phenol oxidation, even in the absence of UV_{254}

Fig. 3. (Color online.) FT–IR spectra for the raw clay, the iron pillared clay and the Cu-doped pillared clay.
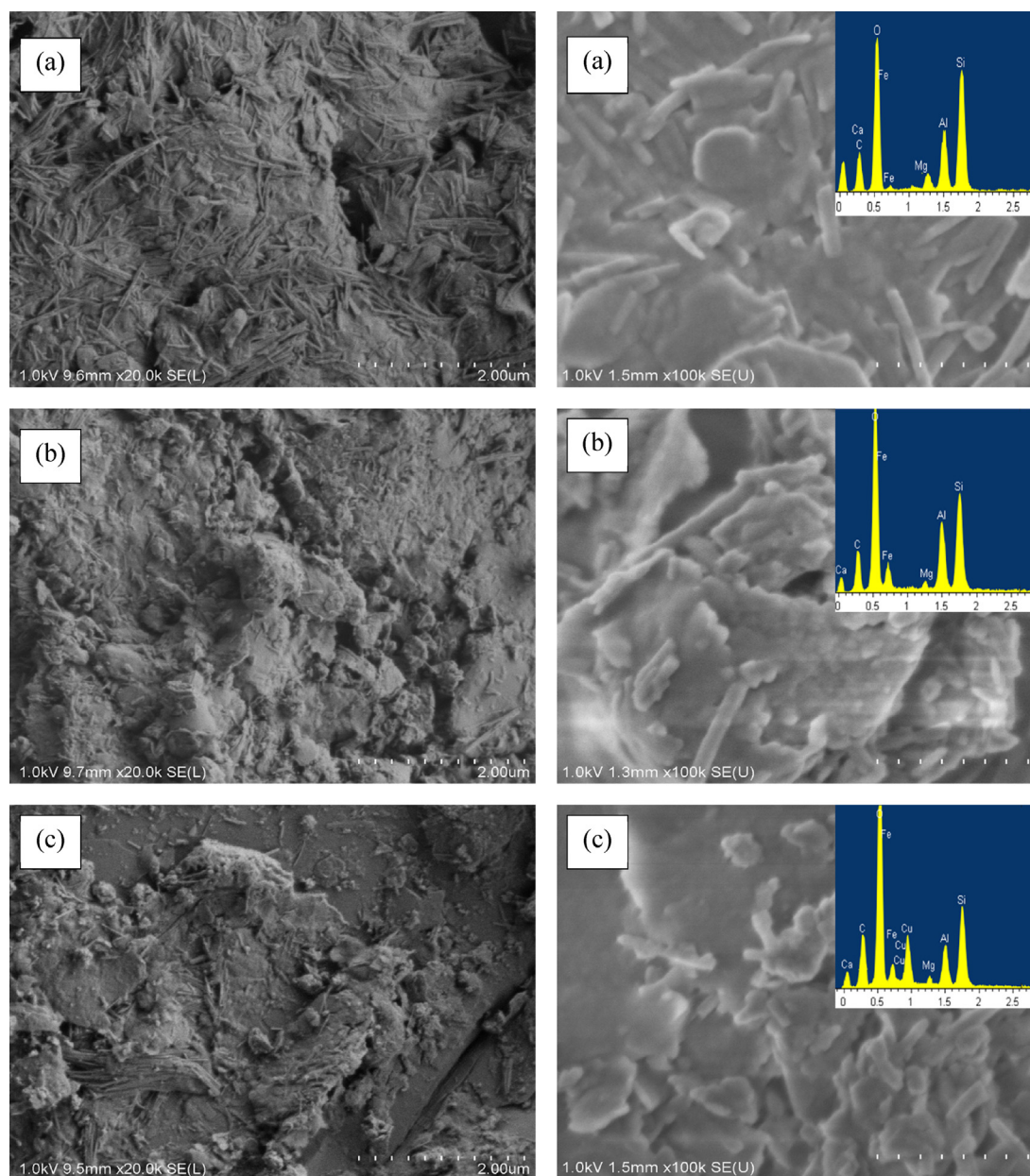
Fig. 4. (Color online.) SEM images and EDX spectra for (a) the raw clay, (b) the iron pillared clay, and (c) the Cu-doped pillared clay.

irradiation. The highest conversion of phenol, close to 100% after 20 min of reaction, was found however when phenol was degraded in the presence of the catalyst, the oxidant H_2O_2, and UV_{254} irradiation, curve (e). For the sake of comparison, let us note here that considerably lower conversions, even at higher H_2O_2 dosages, were measured during phenol oxidation in the presence of the iron pillared clay, Fe–PILC [11], i.e. 60 min of irradiation were needed to complete phenol conversion instead of 30 min (see curve (e) in Fig. 5), pointing to a positive effect of the presence of Cu as the active phase in the Cu/Fe–PILC catalyst.

It is well known that the complete oxidation, i.e. mineralization, of phenol occurs through the formation of

several reaction intermediates, such as *p*-benzoquinone (yellow), *o*-benzoquinone (red), and hydroquinone (colorless) and/or maleic and other carboxylic acids, some of them being even more toxic than phenol itself [28,29]. Mineralization of phenol was thus evaluated through total organic carbon (TOC) measurements and HPLC chromatography. Fig. 6 shows the results of phenol mineralization, measured by means of TOC analyses, for the same reaction conditions as those depicted in Fig. 5. These results evidence first that phenol cannot be mineralized in the sole presence of UV_{254} irradiation, curve (a), or the catalyst Cu/Fe–PILC, curve (b). Mineralization is clearly enhanced in the presence of H_2O_2, curves (c) and (d). Almost 100%
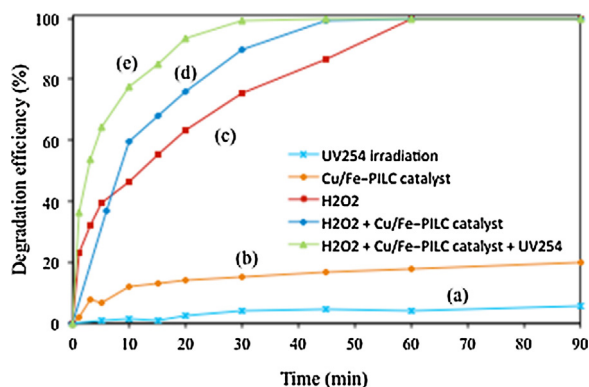
Fig. 5. (Color online.) Phenol degradation measured by means of gas chromatography, initial phenol concentration: 150 mg/L, catalyst loading: 0. 8 g/L, amount of H_2O_2: 3 mL, and pH: 5.05, under different experimental conditions: (a) UV_{254} irradiation, (b) Cu/Fe–PILC catalyst, (c) H_2O_2, (d) H_2O_2 + Cu/Fe–PILC catalyst, and (e) H_2O_2 + Cu/Fe–PILC catalyst + UV_{254} irradiation.
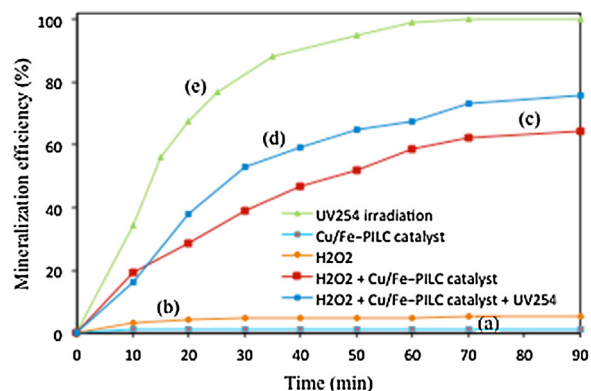
Fig. 6. (Color online.) Phenol mineralization measured by means TOC analyses, initial phenol concentration: 150 mg/L, catalyst loading: 0.8 g/L, amount of H_2O_2: 3 mL, and pH: 5.05, under different experimental conditions: (a) UV_{254} irradiation, (b) Cu/Fe–PILC catalyst, (c) H_2O_2, (d) H_2O_2 + Cu/Fe–PILC catalyst, and (e) H_2O_2 + Cu/Fe–PILC catalyst + UV_{254} irradiation.

TOC, i.e. total mineralization of phenol, can be obtained after 60 min of reaction in the presence of the Cu/Fe–PILC catalyst, H_2O_2, and UV_{254} irradiation, curve (e).

In addition, HPLC chromatography evidences that the initial single peak of phenol appearing at retention times of about 5.5 min (Fig. 7, peak 1) is decomposed into two new peaks at 2.2 and 4.9 min (peaks 2 and 3), after 30 min of

reaction, in the presence of either H_2O_2 or the Cu/Fe–PILC. Both solutions show a certain brownish color, which is in agreement with the observations of Mijangos et al. [29], and may point to the presence of p-benzoquinone and/or o-benzoquinone intermediates. The solution after 30 min of oxidation in the presence of H_2O_2, UV and the Cu/Fe–PILC catalyst looks completely colorless, almost all peaks
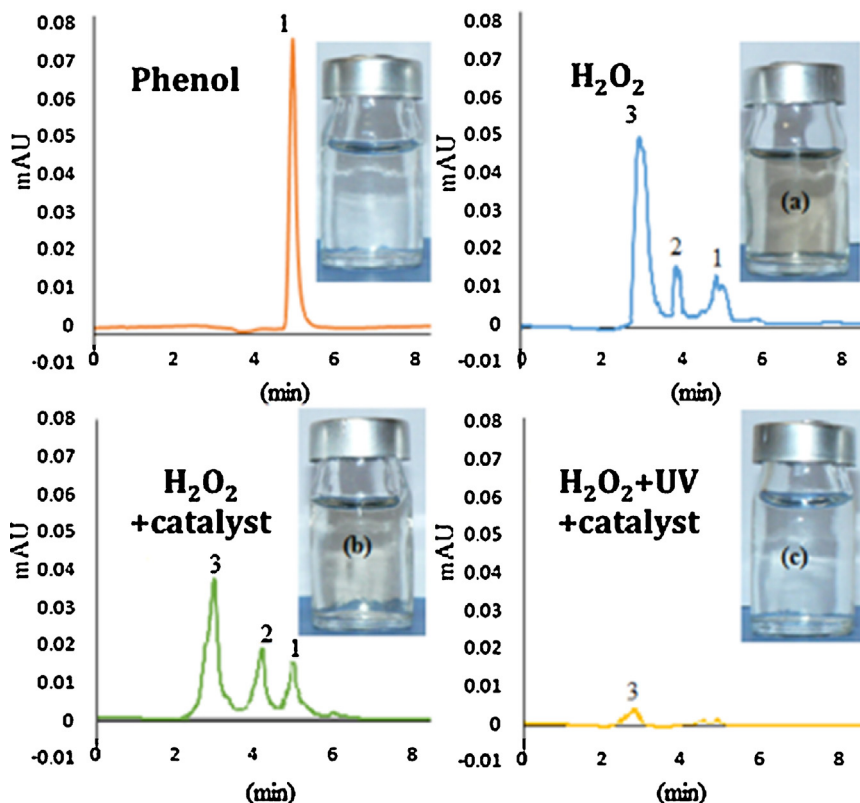

Fig. 7. (Color online.) HPLC chromatograms for the initial phenol solution and the products of reaction after 30 min of reaction, in the presence of H_2O_2, H_2O_2 + Cu-doped pillared clay, and H_2O_2 + UV + Cu-doped pillared clay, together with the pictures taken for each one of these solutions.
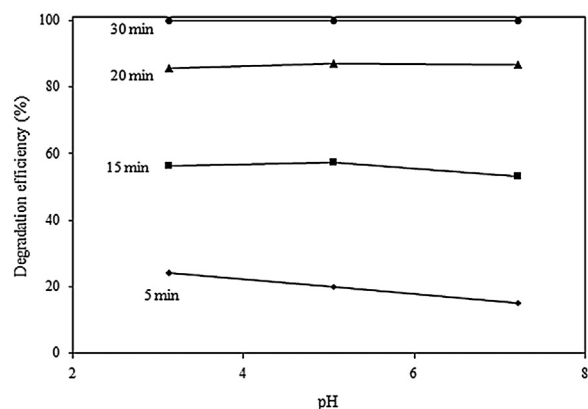
Fig. 8. Influence of the initial solution pH in the photo-Fenton degradation of phenol, at initial phenol concentration: 150 mg/L, catalyst loading: 0. 8 g/L, H_2O_2 concentration: 0.44 mmol/L.

practically disappear from the HPLC chromatogram, and only small amounts of the low-molecular-weight acids can be considered to be present.

3.3. Influence of reaction conditions on photo-Fenton phenol oxidation in the presence of the Cu/Fe–PILC catalyst

The influence of the pH of the initial phenol solution on the photo-Fenton activity of the Cu/Fe–PILC catalyst was tested at pHs 3.1, 5.1 and 7.2. The results are presented in Fig. 8 and evidence that the variation of the solution pH has practically no influence on the measured degradation of phenol. Similar observations have also been recently reported in the literature about the ability of Cu-based catalysts to generate •OH in what is referred to as a Fenton-like process over a wide range of pH [12,14,16].

The H_2O_2 dosage is a crucial factor affecting the generation of •OH radicals, therefore conditioning the efficiency of the photo-Fenton-like degradation process. Fig. 9 shows the results of the photo-Fenton experiments carried out for H_2O_2 dosages from 2 mL to 7 mL, at a pH of 5.1, in the presence of 0.8 g/L Cu–Fe–PILC and UV_{254} irradiation. The results point to the presence of an optimal oxidant dosage. Excess amounts of H_2O_2 can act in fact as

an •OH scavenger resulting in the generation of perhy-droxyl radicals ($HO_2^•$), see Eq. (2) and (3), a less strong oxidant as compared to hydroxyl radicals [15,16]:

$$H_2O_2 + HO^• \rightarrow HO_2^• + H_2O \tag{2}$$

$$HO^• + HO_2^• \rightarrow O_2 + H_2O \tag{3}$$

The effect of the catalyst's dosage was evaluated by means of varying its concentration from 0.1 to 1.5 g/L (Fig. 10). Phenol conversion increases for increasing Cu/Fe–PILC concentrations in the range 0.1–0.6 g/L. Together with enhanced adsorption occurring to a higher extent when a higher catalyst loading is used, increased phenol degradation is due to the increase of the accessible number of surface active sites resulting in an enhanced free hydroxyl radical generation [16]. Conversion is stabilized for catalyst dosages in the range 0.6–0.8 g/L, decreasing notably for higher initial catalyst concentrations. Excess of catalyst leading to substantial particle agglomeration may explain this fact, together with the more difficult diffusion of the UV irradiation through a more opaque suspension.

The performance of photo-Fenton oxidation processes is strongly affected by the wavelength of the light employed. It has been reported that degradation occurs more efficiently in the presence of UV_{254} irradiation (UV-C, $\lambda = 254$ nm) than in the presence of UV_{365} irradiation (UV-A, $\lambda = 365$ nm) [11,30]. Moreover, the generation of oxidation intermediates, i.e. carboxylic acids, may result in a decrease of the solution pH that can contribute to increased metal leaching [31]. Fig. 11 presents the results of two different experiments performed either in the presence of UV-C or UV-A. Phenol degradation efficiency decreases when using UV-A light, $\lambda = 365$ nm, in comparison to the experiment performed in the presence of UV-C, $\lambda = 254$ nm. However, under UV-C, a degradation efficiency of 100% can be still attained after longer reaction times, i.e. 60 min of reaction. The degradation is moreover accompanied by a decrease in the solution pH, which occurs faster in the presence of UV-C. In spite of this, the concentrations of leached metals, iron and copper, remain considerably low, from 0 to 0.27 or 0.16 ppm respectively (analyzed in
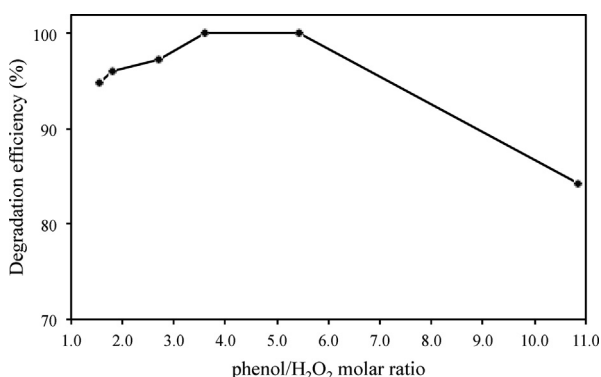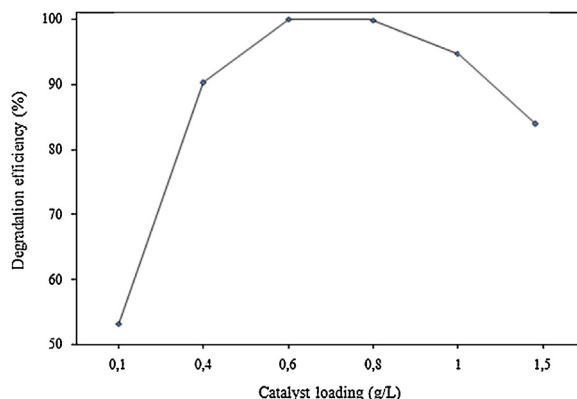

Fig. 9. Influence of the H_2O_2 dosage in the photo-Fenton degradation of phenol, at initial phenol concentration: 150 mg/L, pH: 5.1 and catalyst loading: 0. 8 g/L, upon 60 min of irradiation.

Fig. 10. Influence of catalyst concentration in the photo-Fenton degradation of phenol, at initial phenol concentration: 150 mg/L, pH: 5.1 and H_2O_2 concentration: 0.44 mmol/L, upon 60 min of irradiation.
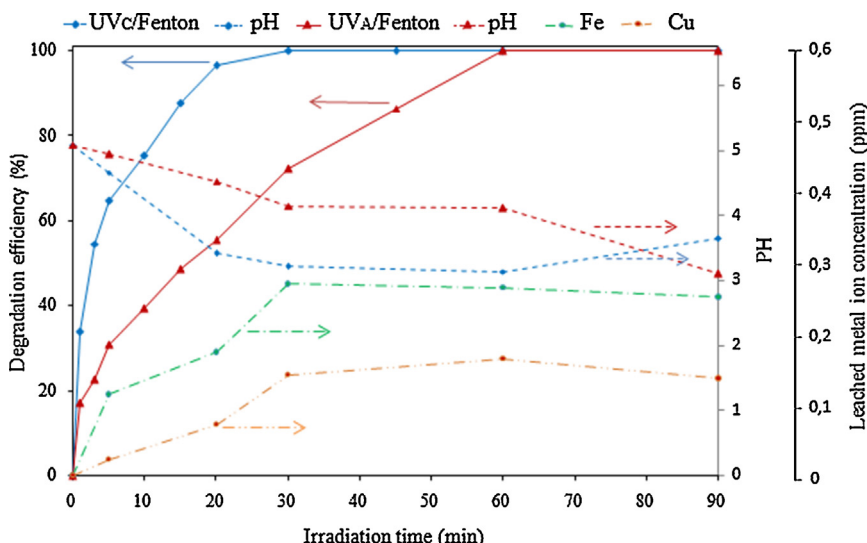
Fig. 11. (Color online.) Phenol degradation efficiency measured under UV-C and UV-A light, evolution of pH during reaction, together with Fe and Cu concentrations measured during the photo-Fenton experiments at initial phenol concentration: 150 mg/L, pH: 5, 0.8 g/L catalyst loading and H_2O_2 concentration: 0.44 mmol/L.

the resulting solution by means of ICP-OES). Let us note here that three successive cycles, each one of a duration of 90 min, were performed by reusing the same catalyst. The loss of activity was found to be negligible, around 2%, which may even fall within the experimental error. Together with the extremely low amounts of metal leached through the reactions, this fact points to the high stability of the Cu-doped Fe-pillared clays prepared and presented in this work.

4. Conclusions

A Cu-doped Fe-pillared clay was synthesized from a local Tunisian clay and tested for phenol oxidation under photo-Fenton conditions. Its physicochemical characterization pointed to successful pillaring and incorporation of Cu into the clay structure. Iron was found to be present both in the forms of magnetite and hematite, whereas no reflections corresponding to Cu oxides were observed in the XRD patterns, pointing to the presence of these compounds at very small crystal sizes, i.e. highly dispersed on the clay surface. XRF analyses confirmed, however, the presence of the Cu species and its successful incorporation into the clay pillars.

Photo-Fenton experiments in the presence of this Cu/Fe–PILC evidenced its considerable activity towards the selective oxidation of phenol. Complete mineralization, confirmed by means of TOC and HPLC analyses, of this toxic compound was attained after 40 min of reaction, in the presence of UV-C irradiation.

The photo-Fenton reaction was found to be sensitive to several operational parameters, such as the concentration of H_2O_2 and catalyst dosage. In both cases, an optimal concentration of both the oxidant and the catalyst was found at 2–3 mL – around 0.4 mmol/L – of H_2O_2 and 0.6–0.8 g/L of catalyst. The catalyst was however active over a wide range of pH, from 3 to 7, without observing noticeable changes in its activity. Phenol degradation efficiency

decreased when using UV-A light instead of UV-C. Total degradation was still possible after longer reaction times, i.e. 60 min. Negligible leaching of iron and copper was found during the test, with maximal concentrations of the metals well below 0.5 ppm. Catalyst was reutilized in three successive reaction cycles without observing any remarkable decrease in its activity.

References

[1] ATSDR, ToxFAQs™ for phenol., 2008 http://www.atsdr.cdc.gov/.
[2] M. Weber, M. Weber, M. Kleine-Boymann, Phenol, in: Ullmann's Encyclopedia of Industrial Chemistry, John Wiley & Sons, 2008.
[3] G. Busca, S. Berardinelli, C. Resini, L. Arrighi, J. Hazard. Mater. 160 (2008) 265.
[4] E. Neyens, J. Baeyens, J. Hazard. Mater. 98 (2003) 33.
[5] S. Parsons, Advanced Oxidation Processes for Water and Wastewater Treatment, IWA, London, 2004.
[6] C. Walling, Acc. Chem. Res. 8 (1975) 125.
[7] S.A. Wang, Dyes Pigments 76 (2008) 714.
[8] J. Herney-Ramirez, A.V. Miguel, M.M. Luis, Appl. Catal. B: Environ. 98 (2010) 10.
[9] A.N. Soon, B.H. Hameed, Desalination 269 (2011) 1.
[10] S. Navalon, M. Alvaro, H. Garcia, Appl. Catal. B Environ. 99 (2010) 1.
[11] H. Belhadjltaief, P. Dacosta, P. Beaunier, M. Elena Galvez, M. Benzina, Appl. Clay Sci. (2014) 46.
[12] R. Benachma, A. Ghorbel, A. Dafinov, F. Medina, J. Phys. Chem. Sol. 73 (2012) 1524.
[13] R. Benachma, A. Ghorbel, A. Dafinov, F. Medina, Appl. Catal. A 349 (2008) 20.
[14] A.C.K. Yip, F.L.Y. Lam, X. Hu, Ind. Eng. Chem. Res. 44 (2005) 7983.
[15] A.C.K. Yip, F.L.Y. Lam, X. Hu, Chem. Commun. 25 (2005) 3218.
[16] O.B. Ayodele, B.H. Hameed, J. Ind. Eng. Chem. 19 (2013) 966.
[17] M.N. Timofeeva, S.Ts. Khankhasaeva, E.P. Talsi, V.N. Panchenko, A.V. Golovin, E.Ts. Dashinamzhilova, S.V. Tsybulya, Appl. Catal. B: Environ. 90 (2009) 618.
[18] H. Belhadjltaief, P. Dacosta, M. Elena Galvez, M. Benzina, Ind. Eng. Chem. 52 (2013) 16656.

[19] O.B. Ayodele, J.K. Lim, B.H. Hameed, Appl. Catal. A 413 (2012) 301.
[20] J. Feng, X. Hu, P.L. Yue, H.Y. Zhu, G.Q. Lu, Water Res. 37 (2003) 3776.
[21] J. Feng, X. Hu, P.L. Yue, H.Y. Zhu, G.Q. Lu, Chem. Eng. Sci. 58 (2003) 679.
[22] X. Li, G. Lu, Z. Qu, D. Zhang, S. Liu, Appl. Catal. A: Gen. 398 (2011) 82.
[23] J.G. Carriazo, Appl. Clay Sci 67 (2012) 99.
[24] F.G.E. Nogueira, J.H. Lopes, A.C. Silva, R.M. Lago, J.D. Fabris, L.C.A. Oliveira, Appl. Clay Sci. 51 (2011) 385.
[25] F. Martínez, G. Calleja, J.A. Melero, R. Molina, Appl. Catal. B: Environ. 70 (2007) 452.
[26] F.G.E. Nogueira, J.H. Lopes, A.C. Silva, M. Gonçalves, A.S. Anastácio, K. Sapag, L.C.A. Oliveira, Appl. Clay Sci 43 (2009) 190.
[27] F. Tomul, Appl. Surf. Sci. 258 (2011) 1836.
[28] M.S. Yalfani, S. Contreras, F. Medina, J. Sueiras, Appl Catal. B: Environ. 89 (2009) 519.
[29] F. Mijangos, F. Varona, N. Villota, Environ. Sci. Technol. 40 (2006) 5538.
[30] B. Iurascu, I. Siminiceanu, D. Vione, M.A. Vicente, A. Gil, Water Res. 43 (2009) 1313.
[31] W.M. Wang, J. Song, X. Han, J. Hazard. Mater. 262 (2013) 412.